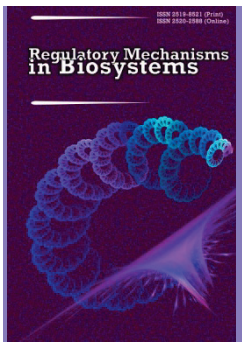

Regulatory Mechanisms in Biosystems

ISSN 2519-8521 (Print)
ISSN 2520-2588 (Online)
Regul. Mech. Biosyst.,
2023, 14(1), 86–93
doi: 10.15421/022313

The effect of $GdYVO_4:Eu^{3+}$ nanocrystals on the intercellular adhesion of mesenchymal stem cells *in vitro*

Y. H. Kot*, K. V. Kot*, N. S. Kavok**, V. K. Klochkov**

**V. N. Karazin Kharkiv National University, Kharkiv, Ukraine*
***Institute for Scintillation Materials, Kharkiv, Ukraine*

Article info

Received 21.01.2023
Received in revised form 16.02.2023
Accepted 17.02.2023

V. N. Karazin Kharkiv National University, Svobody Sq., 4, Kharkiv, 61022, Ukraine. Tel.: +38-093-973-17-73. E-mail: yurii.kot@karazin.ua

Institute for Scintillation Materials, Nauky ave., 60, Kharkiv, 61072, Ukraine. Tel.: +38-097-407-27-84. E-mail: kavok@isma.kharkov.ua

Kot, Y. H., Kot, K. V., Kavok, N. S., & Klochkov, V. K. (2023). The effect of $GdYVO_4:Eu^{3+}$ nanocrystals on the intercellular adhesion of mesenchymal stem cells in vitro. Regulatory Mechanisms in Biosystems, 14(1), 86–93. doi:10.15421/022313

Adult stem cells, such as MSCs, spontaneously differentiate *in vitro*. This makes it difficult both to study this important cell type and to grow large numbers of MSCs for clinical use. While conventional cell cultivation methods cannot cope with this problem, nanostructured materials science offers hope. The effect of small-sized spherical nanoparticles based on orthovanadates of rare-earth elements activated by europium ($GdYVO_4:Eu^{3+}$ nanoparticles, diameter 1–2 nm) on cell-cell adhesion of rat bone marrow mesenchymal stem cells (rBM-MSCs) *in vitro* was studied using electrophoretic separation of proteins, immunofluorescence and confocal laser scanning microscopy. Our study revealed that rBM-MSCs treated with small-sized $GdYVO_4:Eu^{3+}$ nanoparticles had a significant impairment of intercellular adhesion *in vitro*. The pre-incubation of mesenchymal stem cells of rat bone marrow with $GdYVO_4:Eu^{3+}$ nanocrystals at a non-toxic concentration of 0.5 μg/mL during 1 hour of cultivation did not lead to significant changes in cell monolayer, the number of cells and the area of cell bodies did not change. However, the density of the monolayer and the area of the cell field decreased after the incubation. The incubation of cells with nanoparticles led to an increase in the area of the intercellular gate – a location of disruption of cell adhesion, compared to cells without nanoparticles in culture medium. The pre-incubation of rBM-MSCs with nanocrystals caused no changes in the content of total cadherins in the plasma membrane; a decrease in the content of cytoplasmic calreticulin and an increase in the content of surface calreticulin; a decrease in the content of free calcium in the cytoplasm, and an increase in protein-bound intercellular calcium and calcium in the extracellular space. The colocalization analysis revealed that the colocalization of calreticulins with cadherins on the outer surface of the plasma membrane of cells significantly increased after the incubation with $GdYVO_4:Eu^{3+}$ nanocrystals. The paper proposes a possible mechanism of reducing the degree of adhesion by nanocrystals. This study emphasizes the possibility of modulating MSCs adhesion using $GdYVO_4:Eu^{3+}$ nanoparticles. The development of new technologies capable of mitigating adhesion is crucial for the development of regenerative strategies using stem cells.

Keywords: MSCs; gadolinium orthovanadate nanoparticles; adhesion; cadherins; calreticulins; calcium.

Introduction

Adult stem cells, such as mesenchymal stem cells (MSCs), differentiate spontaneously *in vitro* (Gimble et al., 2008). Therefore, MSCs change the direction of differentiation in response not only to specific differentiation-inducing chemical factors in the culture medium, but also in response to the stiffness of the environment surrounding the cells and the nanostructure of a substrate (Yang et al., 2018). Numerous studies have been conducted to control the direction of differentiation based on the interaction between MSCs and culture substrate (Miyoshi & Adachi, 2014; Wang et al., 2016). In mesenchymal stem cells cultured in a monolayer, adipogenesis is promoted by cell-cell contact (due to high density), whereas osteogenesis is inhibited by cell-cell contact due to the subsequent reduction of cell-extracellular matrix contact area (Mao et al., 2016; Robert et al., 2020). Homotypic intercellular contact is important because increased cell-to-cell contacts between MSCs regulate gene differentiation regardless of substrate stiffness (Tang et al., 2010; Xue et al., 2013). The seeding density of MSCs was observed to affect the response to mechanical signals depending on intercellular contacts with cells seeded at high densities, promoting spontaneous differentiation (Zhao et al., 2020). Mareschi and colleagues evaluated the impact of initial cell density and the time of culture on morphology, metabolic activity, and differentiation potential of BM-MSCs. Their studies revealed that optimal cell growth occurs at a lower culture density and cell-cell adhesion. A culture of MSC derived from high cell plating densities resulted in an increased number of flat cells with non-normal morphology and low proliferation rate (Mareschi et al., 2012; Drela et al., 2019).

The conventional methods of cell cultivation cannot cope with this problem. The growth and expansion of rBM-MSCs and other adherent cells in general rely on interactions with soluble components in the culture medium and the surrounding cells. Accordingly, MSC expansion, cell-cell and cell-substrate adhesion in vitro have been enhanced by fortifying culture media with exogenous soluble factors and/or by coating culture surfaces with extracellular matrix components or synthetic biocompatible polymers (Anderson et al., 2016; Lu et al., 2022). While Fraire et al. (2020) found that improper long-time cultivation could induce premature senescence of MSCs, others demonstrated that MSCs cultured on poly-L-lysine-coated plates could reverse the replicative senescence, but a high concentration of PLL was toxic (Lu et al., 2009). Another study indicated that hBM-MSCs embedded in type I collagen microspheres exhibited increased cell-cell adhesion and chondrogenic matrix accumulation in vitro (Mathieu et al., 2014). The xenogeneic-free type I collagen-based recombinant peptide substrate (PCP) can support more efficient and safer scalable culture systems for the production of MSCs, but the inclusion of RCP in the culture medium enhances cellular adhesion (Muraya et al., 2019). After cultivation on hyaluronic acid (HA)-based, cell-adhesive

hydrogels (HA-gHGP), type I collagen production and mineral deposition were detected in absence of osteogenic supplements in culture media, suggesting induction of spontaneous osteogenic differentiation (Jha et al., 2011). Tropoelastin, both as an immobilized substrate and as a soluble additive, drives proliferation and phenotypic maintenance of mesenchymal stem cell but elicits immediate strong mitogenic and cell-attractive responses (Yeo & Weiss, 2019). Some natural proteins, such as silk fibroin, cellulose, and decellularized extracellular matrix demonstrate a balance among mechanical strength, toughness, and elasticity, controllable slow degradation rate, and good biocompatibility but time-consuming cell harvest process (Chen, 2022). In mesenchymal cells, intercellular contact is mediated through the homotypic calcium-dependent interaction of cadherins on adjacent cells. Cadherin contains both an extracellular domain that mediates this adhesion, and a cytosolic domain that acts as a signaling hub and anchor that couples with the actin cytoskeleton (Zhang et al., 2020). The separation force between adhering cells was shown to depend on the cadherin concentration on the surface (Montel et al., 2022).

The development of new technologies capable of mitigating adhesion is critical to the development of regenerative strategies using stem cells. Nanostructured materials science offers hope to control cell-cell adhesion and spontaneous differentiation *in vitro*. The studies demonstrated that the suppression of cell spreading caused by nanoscale structures can downregulate the progress of osteogenic differentiation (Yamazaki et al., 2020). The migratory activity of hBM-MSCs decreased significantly after SiO_2(RITC) nanoparticles treatment, but compared with such of the control, the viability of SiO_2(RITC)-treated hBM-MSCs decreased by 10% and intracellular ROS increased by two times (Shin et al., 2019). Wang et al. (2009) observed that single-walled carbon nanotubes (SWCNTs) can inhibit human embryonic kidney cell line proliferation, and decrease cell adhesive ability in a dose- and time-dependent manner, but SWCNTs inhibit cell growth by inducing cell apoptosis. Unique biological properties of nanoparticles based on rare-earth metals such as antioxidants and anti-inflammatory nature suggest that this type of nanomaterials is an appropriate biomaterial for cell technologies and bioengineering applications (Li et al., 2018; Natarajan et al., 2022).

Materials and methods

For the study, we used cells obtained from the bone marrow of 3-month-old (140–160 g) Wistar male laboratory rats. The rats were housed under standard conditions in animal rooms at 21 ± 2 °C, 50 ± 10% of humidity, and a 12-h light/dark cycle (Garber et al., 2011). All the studies on animals were carried out in accordance with the requirements of the Domestic Legislation, the Law of Ukraine "On Protection of Animals against Abuse" No. 3447-IV as of 21.02.2006, last amended on 08.04.2017, and Directive 2010/63/EU of the European Parliament and of the Council. Bone marrow aspirate was obtained from femurs of rats (n = 4), which were euthanized with an overdose (50 mg/kg) of sodium thiopental (Brovapharma, Ukraine). Every effort was made to minimize the number of animals used in the experiment and their discomfort.

The cell suspensions were collected by flushing the marrow cavity with 199 Medium (Biowest, France), filtered through a 40 μm nylon screen insert (Biologix, Germany), and centrifuged at 300 g for 10 min in a Durafuge 200 centrifuge (Thermo Scientific, USA). The cell pellets were resuspended in Dulbecco's PBS (Gibco, USA). The total number of the nucleated cells and viability in primary suspension were counted on a Countess II FL counter (Invitrogen, USA) using the "Ready Count Green/Red Dead Viability Stain Kit" (Cat. A49905, Invitrogen, USA). The mean viability of the cells in primary suspension was 91.0 ± 0.5%.

As known, CD90 (Thy-1) is a cell surface glycoprotein heterogeneously expressed in rBM-MSCs (Zhang & Chan, 2010). Thy-1-positive cells were separated by immunomagnetic separation using CD90/Thy1 antibody [7E1B11] (ab181469, Abcam, UK), EasySep™ Rat Custom Positive Selection Kit immunomagnetic kit (Stemcell Tec., Germany), and a DynaMag™ Magnet (Invitrogen, USA) as described by the manufacturer.

Thy-1-positive cells were seeded in the density of 1.5·104 cells/well in a Millicell EZ SLIDE 8 (Merck Millipore, USA) well glass slide and allowed to grow in medium αMEM supplemented with L-glutamine 2 mM (Biowest, France), fetal bovine serum 15% (Gibco, USA) and 1% "Antibiotic-Antimycotic Solution" (Gibco™, USA) using a Galaxy 14S (Eppendorf, Germany) CO_2-incubator (37 ºC, 96% RH, and 5% CO_2) for 4 days until 80–85% confluence. The non-adherent cells were removed in 48 h incubation after the first medium change.

The MSC identity of the isolated cells was confirmed by the ability of the cells to adhere to plastic, form colonies under the standard culture conditions, and differentiate into adipocytes and osteoblasts in an induced culture medium (Dominici et al., 2006). Besides that, rBM-MSCs were tested for mycoplasma contamination using the "MycoAlert® Mycoplasma Detection Kit" (Lonza Inc., Switzerland) and a Sirius L luminometer (Titertek Berthold, USA). All the experiments were performed using cells in their three passages.

In this study, we used small-sized gadolinium orthovanadate nanoparticles doped with Eu^{3+} ($GdYVO_4$:Eu^{3+} nanoparticles, diameter 2–3 nm) for managing cell-cell adhesion of MSCs. Spherical nanoparticles of $GdYVO_4$:Eu^{3+} (diameter 2–3 nm) were synthesized in the Nanostructured Materials Department named after Y. V. Malyukin, the Institute for Scintillation Materials of National Academy of Sciences of Ukraine. An aqueous colloidal solution of $GdYVO_4$:Eu^{3+} nanoparticles was obtained using the method reported earlier (Klochkov et al., 2011). The ability to penetrate into cells and autofluorescence properties (excitation 361 nm, emission 618 nm) make them very promising for use in visualization or modulation of the structural and functional state of cells (Tkacheva et al., 2019; Jiménez-Jiménez et al., 2020).

The $GdYVO^4$:Eu^{3+} nanoparticles were added to the nutrient medium one hour before the irradiation until their final concentration in the medium of 0.5 μg/mL. Prior to utilization, the nanoparticle suspension was sterilized by filtration using a 0.22 μm syringe filter (Millipore, USA) and autoclaving. For successful testing, nanoparticles have to be biocompatible and non-toxic. Nanoparticles of $GdYVO_4$:Eu^{3+} in the dose used in this study are non-toxic *in vitro* (Zhu et al., 2019; Prokopiuket al., 2022).

The rBM-MSC monolayers were divided into two groups:

Group 1 – cells without exposure to nanoparticles(n = 72),

Group 2 – cells incubated with nanocrystals (n = 72).

One n corresponds to one well of a Millicell EZ SLIDE (Merck Millipore, USA) slide with a monolayer of cells.

The cells were incubated with nanoparticles for 1hour. After that, the nutrient medium was replaced with nanoparticle-free αMEM supplemented with L-glutamine 2 mM (Biowest, France), 15% fetal bovine serum (Gibco, USA) and 1% "Antibiotic-Antimycotic Solution" (Gibco™, USA). Each group was divided into three parts (for each marker determination). In the first part (n = 24), we determined the contents of cadherins, calreticulins and of free oxygen species. In the second part (n = 24), we measured the degree of cadherins and calreticulins colocalization in fixed cells. In the third part (n = 24), we identified the content of free and bound calcium in live cells.

To determine concentrations of cadherins and calreticulins, the plasma membrane proteins and cytoplasmic proteins were isolated, predicated, and electrophoretically separated using "Qproteome Plasma Membrane Kit" (Qiagen, Germany) and "Novex™ XCell SureLock + Power Ease 500 Electrophoresis System" (Invitrogen, USA). After the electrophoretic separation of plasma membrane proteins, the concentration of total cadherins was determined immunofluorometrically using Anti-pan Cadherin primary antibody (Cat. ab16505, Abcam, UK) and Anti-pan Cadherin secondary antibody [EPR1792Y] Intercellular Junction MarkerAlexa Fluor488 (Cat. ab195202, Abcam, UK). In addition, the concentrations of cell surface and cytoplasmic calreticulins were determined immunofluorometrically using Anti-Calreticulin primary antibody (Cat. ab2907, Abcam, UK) and Anti-Calreticulin secondary antibody [EPR3924] ER MarkerAlexa Fluor 594 (Cat. ab275343, Abcam, UK). The visualization and measurement of fluorescence area and intensity were performed by RED Gel Imaging System (Alpha Innotech, USA) using TotalLab CLIQS 1.3.063 software.

For cadherins and calreticulins colocalization analysis, rBM-MSC were fixed using "Image-iT™ Fixation/Permeabilization Kit" (Invitrogen, USA) prior to staining with Anti-pan Cadherin primary antibody (Cat. ab16505, Abcam, UK), Anti-pan Cadherin secondary antibody [EPR1792Y] Intercellular Junction Marker Alexa Fluor 488 (Cat.

ab195202, Abcam, UK), Anti-Calreticulin primary antibody (Cat. ab2907, Abcam, UK), and Anti-Calreticulin secondary antibody [EPR3924] ER Marker Alexa Fluor 594 (Cat. ab275343, Abcam, UK).

To measure free and protein-bound calcium in live cells, MSCs were washed in an imaging buffer "Live Cell Imaging Solution" (Thermo Scientific, USA) and loaded with fluorescent calcium-sensitive Fura Red AM ratiometric dye by incubation in the imaging buffer containing 5 μM Fura Red AM (Cat. F3020, Life Technologies, USA) for 30 min. Excitation/emission = 405/637 nm was used to determine free Ca^{2+}, and excitation/emission = 473/657 nm was used to detect protein-bound Ca^{2+}.

The concentration of free oxygen species in living cells was determined fluorimetrically using the "Cellular Reactive Oxygen Species Detection Assay Kit (Orange Fluorescence)" (Abcam, United Kingdom).

Fixed and live cell fluorescence visualization and measurement of fluorescence intensity, post-acquisition images processing and colocalization analysis were performed using an FV10i-LIV confocal laser scanning microscope (Olympus, Japan) and cell Sense Dimension software (Olympus, Japan). Cells were observed using the same parameters of lasers and photomultipliers.

The data were compared and evaluated using the Shapiro-Wilk normality test for $n < 30$ ($n = 24$) and the nonparametric Mann-Whitney U-test for two independent groups (each parameter – a separate group) using PAST v. 3.17 software (Oyvind Hammer, freeware license). All the data were presented as mean and standard deviation ($x \pm SD$). The difference between the studied parameters was considered statistically significant at $P < 0.05$.

Results

It was found that incubation with $GdYVO_4:Eu^{3+}$ nanoparticles in the used concentration did not lead to dramatic changes in cell monolayers (Fig. 1). The number of cells and the area of cell bodies underwent no changes, but the density of the monolayer and the area of the cell field decreased after 1 hour of incubation (Table 1).

Table 1
The effect of $GdYVO^4:Eu^{3+}$ nanoparticles
on rBM-MSC morphometric indicators in the monolayer

Parameter	(–) $GdYVO_4:Eu^{3+}$	(+) $GdYVO_4:Eu^{3+}$
The number of cells in the well, $x10^4$	8.4 ± 0.2	8.2 ± 0.3
Monolayer density, %	87.5 ± 2.3	80.6 ± 2.7*
Cell body area, μm^2	237 ± 11	211 ± 15
Cell field area, μm^2	361 ± 14	314 ± 12*

Notes: * indicates significant differences ($P < 0.05$, $n = 24$) compared with the group without incubation (–) with $GdYVO_4:Eu^{3+}$ nanoparticles.

The detected decrease in the density of the monolayer was related to the fact that the incubation of cells with nanoparticles led to increase in the area of the intercellular gate – a location of disruption of cell adhesion, compared with cells without nanoparticles in culture medium (Fig. 2).

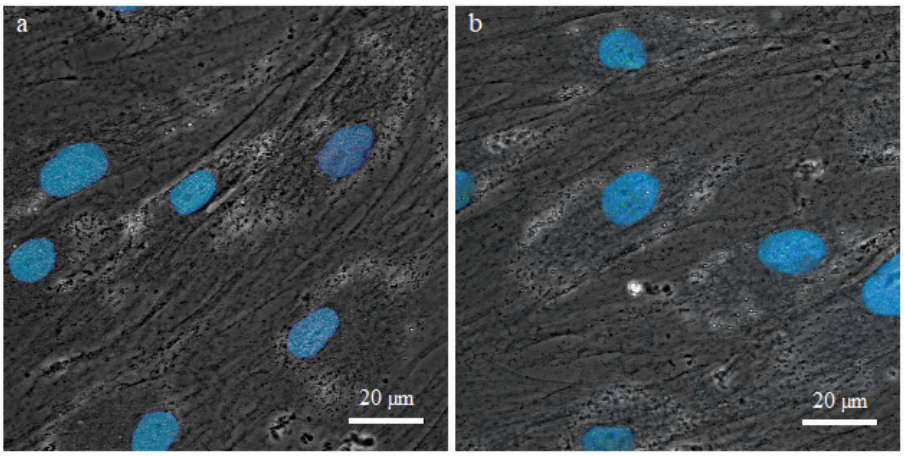

Fig. 1. Confocal laser scanning microscopy (CLSM) visualization (phase contrast and fluorescence modes) of rBM-MSCs monolayer culture without (*a*) and after incubation with nanoparticles (*b*); blue fluorescence is representing nuclei stained by dsDNA-specific dye DAPI (Cat. D1306, Invitrogen, USA); DAPI excitation was provided by 405 nm laser line, and resulting fluorescence was acquired using 461 nm emission line; 60/1.2 NA water-immersion objective

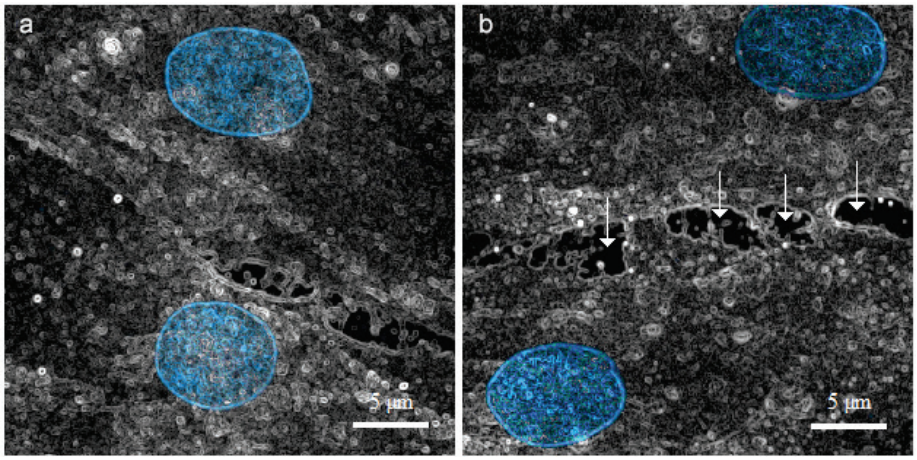

Fig. 2. Confocal laser scanning microscopy (CLSM) visualization (phase contrast and fluorescence modes) of rBM-MSCs monolayer culture without (*a*) and after incubation with nanoparticles (*b*); blue fluorescence is representing nuclei stained by dsDNA-specific dye DAPI (Cat. D1306, Invitrogen, USA); DAPI excitation was provided by 405 nm laser line, and resulting fluorescence was acquired using 461 nm emission line; 60/1.2 NA water-immersion objective; the arrows point to an intercellular gate – a location where disruption of cell adhesion has occurred after the addition of nanoparticles

Figure 3 shows the result of immunofluorescence detection of the fraction of plasma membrane cadherins, as well as the fractions of surface and cytoplasmic calreticulins of mesenchymal stem cells after electrophoretic separation of proteins after 1 hour of incubation with $GdYVO_4:Eu^{3+}$ nanoparticles. The incubation with $GdYVO_4:Eu^{3+}$ nanocrystals did not lead to changes in the content of cadherins in the plasma membrane of rBM-MSCs, but decreased the amount of cytoplasmic calreticulin and increased the content of cell surface calreticulin.

The degree of intercellular adhesion is determined by the interaction of surface calreticulin with plasma membrane cadherins. The detected increase in the specific proportion of surface calreticulin was also confirmed by confocal microscopy data with ratiometric analysis after each protein family was labeled with fluorescent antibodies, as described in the study methods (Fig. 4).

In addition to ratiometric analysis, labeling each family of proteins with fluorescent antibodies made it possible to conduct a colocalization analysis to determine the degree of interaction between plasma membrane cadherins and cell surface calreticulin. The colocalization analysis revealed that the colocalization of calreticulins with cadherins on the outer surface of the plasma membrane of cells significantly increases after incubation with $GdYVO_4:Eu^{3+}$ nanocrystals, as evidenced by a significant increase in the Pearson colocalization coefficient (Fig. 5).

Figure 6 shows the result of determining the content of free calcium and protein-bound calcium in the cytoplasm (*a*) and extracellular space (*b*) of rBM-MSCs culture without (–) and after incubation (+) with nanoparticles. Incubation with $GdYVO_4:Eu^{3+}$ nanoparticles led to a decrease in the content of free and protein-bound calcium in the cytoplasm of cells, and an increase in the content of free and protein-bound calcium in the extracellular space (Fig. 6).

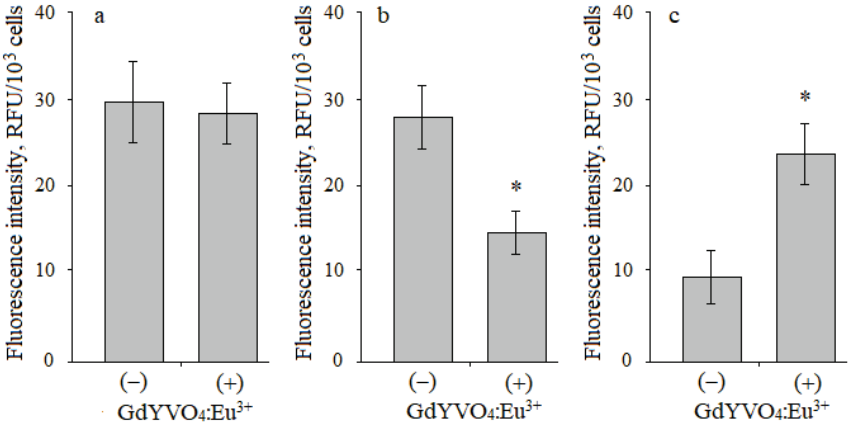

Fig. 3. The content of plasma membrane's total cadherins (*a*), cytoplasmic (*b*) and cell surface (*c*) calreticulins in rBM-MSCs without (–) and after incubation (+) with nanoparticles: * indicates significant differences ($P < 0.05$, $n = 24$) compared with the group without incubation (–) with $GdYVO_4:Eu^{3+}$ nanoparticles

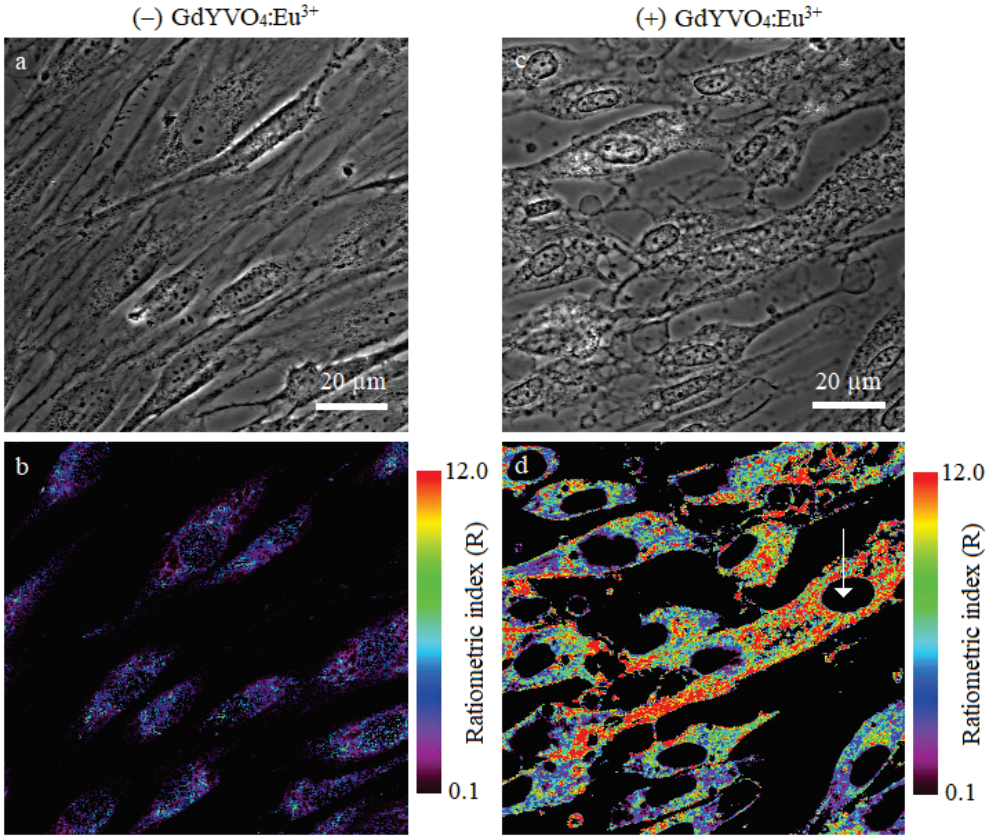

Fig. 4. Confocal laser scanning microscopy (CLSM) phase contrast mode (*a*, *c*) and fluorescence ratiometric mode (*b*, *d*) visualization of rBM-MSCs monolayer culture without (–) and after (+) incubation with nanoparticles: the ratiometric index scale indicates the ratio of the intensities at two excitation wavelengths (cadherins and calreticulin-specific antibodies conjugated with fluorescence dyes Alexa Fluor 488 and Alexa Fluor 594 respectively) and directly correlates with the concentration of both proteins; the arrows point to the nuclei area

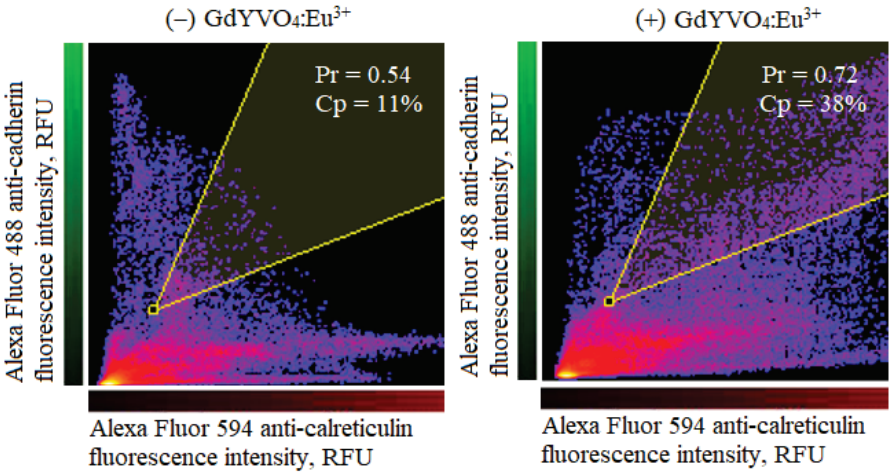

Fig. 5. Data visualization of colocalization analysis of plasma membrane cadherins and cell surface calreticulin of rBM-MSCs monolayer culture without (–) and after (+) incubation with nanoparticles: the Pearson colocalization coefficient (Pr) and percentage of colocalized pixels (Cp) are represented on each image next to the calculated region of interest (indicated in yellow), demonstrating the strength of colocalization based on the fluorescence intensity correlation of cadherins and calreticulin-specific antibodies conjugated with fluorescence dyes Alexa Fluor 488 and Alexa Fluor 594 respectively; * indicates significant differences ($P < 0.05$, $n = 24$) compared to group without incubation (–) with $GdYVO_4:Eu^{3+}$ nanoparticles

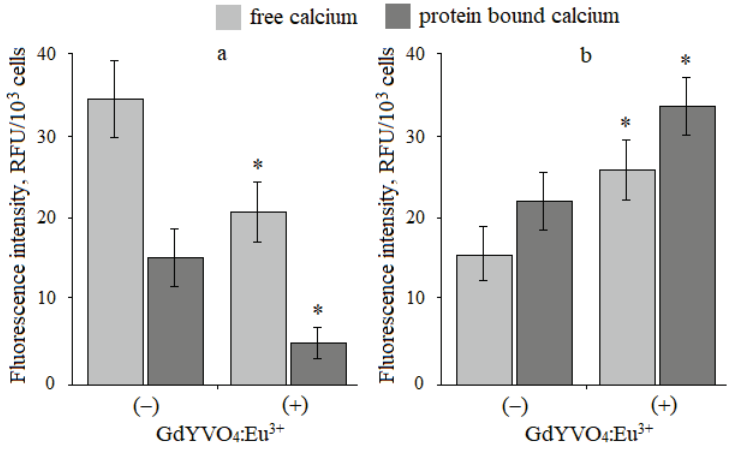

Fig. 6. The content of free calcium and protein-bound calcium in cytoplasm (*a*) and extracellular space (*b*) of rBM-MSCs culture without (–) and after incubation (+) with nanoparticles: * indicates significant differences ($P < 0.05$, $n = 24$) compared with the groups without incubation (–) with $GdYVO_4:Eu^{3+}$ nanoparticles

To reveal the signaling involved in rare-earth orthovanadate nanoparticle-induced effects, the analysis of intracellular reactive oxygen species production was performed, suggesting that no oxidative stress was implicated. It was found that the incubation of rBM-MSCs with $GdYVO_4:Eu^{3+}$ nanocrystals at the concentration of 0.5 μg/mL for 1 hour did not affect the concentration of reactive oxygen species in cells compared with the control group without exposure to nanocrystals (Fig. 7).

Discussion

The decrease in monolayer density and cell field area after 1 hour of incubation with $GdYVO_4:Eu^{3+}$ nanoparticles possibly occurred due to the fact that nanocrystals, which are able to be sorbed on the outer surface of cells (Pakulova et al., 2017; Tkacheva et al., 2019; Bohuslavskyi & Alabedalkarim, 2019), modify their adhesive properties at the level of functional groups of plasma membrane adhesive receptors (mainly integrins and cadherins), such as carboxyl and thiol ones, shielding or inactivating them. In particular, such an effect was described in the literature for gold, iron, and silver nanoparticles in experiments on cell cultures *in vitro* (Sau & Goia, 2012; Shang et al., 2014; Sabourian et al., 2020). Basically, the detected effect is coherent with the data that metal-based nanocrystals are able to inhibit the division and migration of some mammalian cells (Ye et al., 2020; Shariatzadeh et al., 2022; Xu et al., 2022).The revealed decrease in the amount of cytoplasmic calreticulin and the increase in the content of surface reticulin may be a consequence of the activation of calreticulin transport to the outer surface of the plasma membrane by vesicular transport, which is well described in the literature as one of the variants of *in vitro* cell responses to stress, in particular to the effect of various toxicants and metal-based nanoparticles (Owusu et al., 2018; Abdullah et al., 2022; Jody et al., 2022). The detected decrease in the content of free calcium in the cytoplasm and the increase in protein-bound calcium in the extracellular space may be a consequence of the activation of the system of calcium active transport in cells – calcium ATPases, the intensity of which, as known, depends on the physicochemical state of the plasma membrane (Leroueil et al., 2007; Palmgren & Morsomme, 2019), which can change when $GdYVO_4:Eu^{3+}$ nanocrystals contact with the plasma membrane or pass through it (Jiménez-Jiménez et al., 2020; Yaman et al., 2020). Also, xenobiotic-triggered signaling pathways include Ca^{2+} and reactive oxygen species (Liang et al., 2020). Thus, to reveal signaling involved in rare-earth orthovanadate nanoparticle-induced effects, analysis of Ca^{2+} entry and reactive oxygen species (ROS) production was performed to reveal that, unexpectedly, no oxidative stress was implicated. In contrast, it was shown that Ca^{2+} signaling is activated even in response to non-cytotoxic concentrations of metals-based nanoparticles (Zhou et al., 2022). Notably, oxidative stress, including such induced by metal-based magnetic nanoparticles, is known to promote Ca^{2+} entry, and subsequent cell shrinkage (Han et al., 2022). However, our findings indicate that $GdYVO_4:Eu^{3+}$ nanoparticles-induced Ca^{2+} entry did not depend on redox pathways. Although ROS signals are typically associated with cellular injury, these signaling pathways are also critical for maintaining homeostasis. An important component of ROS signaling pertains to localization and tightly regulated signal transduction events within the microenviron-

ments of the cell. One major aspect of this specificity is ROS compartmentalization within membrane-enclosed organelles such as redoxosomes (redox-active endosomes). Redoxosomes can control redox-dependent effector functions through the spatial and temporal regulation of ROS as second messengers (Netanya & Engelhardt, 2014). The incubation of rBM-MSCs with nanoparticles was found to have no effect on the ROS-dependent intensity of fluorescence and amount of redox-active endosomes in the cytoplasm (Fig. 7).

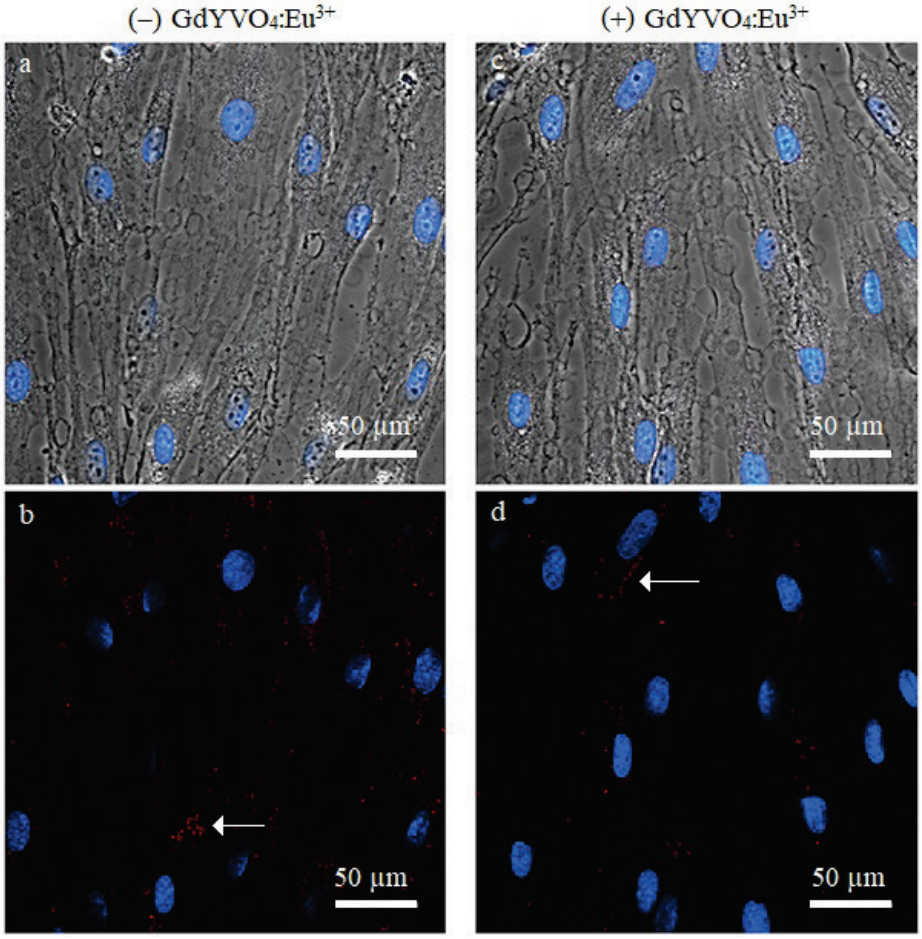

Fig. 7. Confocal laser scanning microscopy (CLSM) phase contrast mode (*a*, *c*) and fluorescence mode (*b*, *d*) visualization of intracellular reactive oxygen species (ROS) in rBM-MSCs monolayer culture without (–) and after (+) incubation with nanoparticles: red fluorescence is representing ROS (Cat. ab186028, Abcam, UK); ROS excitation was provided by 540 nm laser line, and the resulting fluorescence was achieved using 570 nm emission line; blue fluorescence represents nuclei stained by dsDNA-specific dye DAPI (Cat. D1306, Invitrogen, USA); DAPI excitation was provided by 405 nm laser line, and the resulting fluorescence was obtained using 461 nm emission line; 60/1.2 NA water-immersion objective; the arrows point to redox-active redoxosomes

Features of cellular uptake of rare-earth orthovanadate nanoparticles by MSCs may shed light on their cell-cell adhesion inhibition effects. There is evidence that the size of nanoparticles can directly affect their interaction with cells (Pastore, 2021). A model simulating the receptor-mediated endocytosis of nanoparticles of different sizes and shapes demonstrated that the size of the nanoparticles was essential for endocytosis to take place. Specifically, with spherical nanoparticle size ~ 2 nm (as used in the present article), endocytosis occurred faster compared with the nanoparticles of larger sizes (Manzanares & Ceña, 2020). The nanoparticles measuring 2 nm did not induce significant structural changes in the lipids bilayer and achieved maximum permeability. It is believed that the major mechanism of cellular uptake for small nanoparticles is pinocytosis (Foroozandeh & Aziz, 2018). It has been reported that rod-shaped nanoparticles are characterized by lower internalization degree compared with spherical ones (Kapate et al., 2021). Moreover, the accumulation of nanoparticles around cells and their greater stimulating effect on intracellular calcium ion levels suggest that mechanical stress-shear could be responsible for the observed effects (Matuła et al., 2016). It is shown, that Ca^{2+} gradient in cells regulated by external mechanical stress-strain (Ebihara et al., 2022) by mechanically stressed cells is mediated by Piezo1 mechanosensitive cation-permeable channels (Pan et al., 2022). In response to Piezo1-mediated Ca^{2+} influx, the Gardos effect, i.e., potassium efflux, is activated, which drives cell shrinkage (Aglialoro et al., 2021). Cell shape and cellular adhesion are controlled by a variety of pathways, many of them regulated by Ca^{2+}-dependent pathways, which depend on Ca-binding proteins such as calreticulins. Calreticulin plays a central role in intracellular Ca homeostasis, including the regulation of store-operated Ca influx via plasma membrane and ER Ca channels. Numerous studies have indicated that alterations in calreticulin levels affect both cell shape and adhesion in a variety of cell types, including stem cells (Alvandi et al., 2021; Iwahashiet al., 2021). Cells that are either underexpressing or lacking calreticulin have impaired cell adhesion, whereas overexpression of calreticulin increases adherens-type adhesion in both cell-substratum and cell-cell varieties (Jiang et al., 2014). However, our findings indicate that the decrease in the area of cell-cell contacts is independent of the increase of surface calreticulin levels in cells after incubation with nanoparticles. It should be noted that mechanisms,whereby calreticulin affects cell adhesiveness are unclear, but certainly, the regulation of expression of adhesion proteins such as vinculin, N-cadherin, and fibronectin plays a crucial role. It was shown that incubation with $GdYVO_4:Eu^{3+}$ nanocrystals does not lead to changes in the content of cadherins in the plasma membrane of rBM-MSCs, but causes decrease in cytoplasmic calreticulin and increase in content of cell surface calreticulin (Fig. 3). It is known that differential expression of calreticulin affects tyrosine phosphorylation of cellular proteins in a reciprocal manner, such that an increased surface calreticulin expression decreases total tyrosine phosphorylation (Alvandi et al., 2020).

The formation of stable cell-cell adhesions by cadherins depends on the association of their cytoplasmic domain with catenin family proteins. The binding of beta-catenin to these partners is regulated by the phosphorylation of tyrosine residues. Tyrosine phosphorylation contributes to the regulation or perturbation of cadherin function (Jin et al., 2022).

Based on the obtained results and the analysis of literature data, a possible mechanism for reducing the degree of intercellular adhesion of rBM-MSCs during incubation with $GdYVO_4:Eu^{3+}$ nanoparticles could be as follows:

1) $GdYVO_4:Eu^{3+}$ nanocrystals interact with cells, being partially absorbed on their surface and passing through the plasma membrane, changing its physical and chemical properties;

2) accumulation of nanoparticles around cells and their higher stimulating effect on intracellular calcium ion levels suggest that the accumulation of nanoparticles causes mechanical stress-shear to cell membrane;

3) mechanical stress-dependent change in the physical and chemical properties of the plasma membrane of cells leads to the activation of the system of active transport of calcium and cytoplasmic calreticulin from the cell;

4) activation of the universal mechanism of vesicular transport of cytoplasmic calreticulin from the cell leads to an increase in its content on the outer surface of the plasma membrane;

5) on the one hand, overexpression of surface calreticulin can act as a competitive inhibitor of calcium binding to cadherins, which can lead to an inhibition of cadherin dimerization (Yui et al., 2021; Maker et al., 2022) and a decrease in the degree of cell-cell adhesion. On the other hand, increased surface calreticulin expression causes decreased total tyrosine phosphorylation and perturbation of cadherin function.

Conclusion

This study found that rBM-MSCs treated with small-sized $GdYVO_4:Eu^{3+}$ nanoparticles exhibited a significant impairment in cell-cell adhesion *in vitro*. The nanocrystals lead to the activation of the calcium transport system from the cell and the calreticulin-dependent response to stress, as a result of which calreticulin is transported to the plasma membrane, where it colocalizes with cadherins and, probably, acts as a competitive inhibitor of calcium, which can lead to inhibition of new contacts and damage to already formed ones. The study emphasizes the possibility of adhesion modulation of rBM-MSCs in order to enable the development of regenerative strategies using stem cells, a better understanding of potential cell therapeutic applications of MSCs through nanotechnology, and in-depth cytotoxic evaluation of nanoparticles supporting their safer use, especially in biomedical applications.

The research was supported by the Fund for Development and Modernization of Educational and Scientific Equipment of V. N. Karazin Kharkiv National University (No. 0304-1/439), Kharkiv, Ukraine.

The authors declare that the research was conducted in the absence of any commercial or financial relationships that could be construed as a potential conflict of interest.

References

Abdullah, T. M., Whatmore, J., & Bremer, E. (2022). Endoplasmic reticulum stress-induced release and binding of calreticulin from human ovarian cancer cells. Cancer Immunology and Immunotherapy, 71, 1655–1669.

Aglialoro, F., Abay, A., Yagci, N., Rab, M., Kaestner, L., van Wijk, R., von Lindern, M., & van den Akker, E. (2021). Mechanical stress induces Ca^{2+}-dependent signal transduction in erythroblasts and modulates erythropoiesis. International Journal of Molecular Sciences, 22(2), 955.

Alvandi, Z., Al-Mansoori, L., & Opas, M. (2020). Calreticulin regulates Src kinase in osteogenic differentiation from embryonic stem cells. Stem Cell Research, 48, 101972.

Anderson, H. J., Sahoo, J. K., Ulijn, R. V., & Dalby, M. J. (2016). Mesenchymal stem cell fate: Applying biomaterials for control of stem cell behavior. Frontiers in Bioengineering and Biotechnology, 13(4), 38.

Bohuslavskyi, K., & Alabedalkarim, N. (2019). Labeling of Pk-15 cell line with nanoparticles of hadolinium orthovanadate: Influence of time and incubation conditions. JMBS, 4(4), 230–236.

Chen, J. (2022). Recent development of biomaterials combined with mesenchymal stem cells as a strategy in cartilage regeneration. International Journal of Translational Medicine, 3, 456–481.

Dominici, M., Blanc, K. L., & Mueller, I. (2006). Minimal criteria for defining multipotent mesenchymal stromal cells. Cytotherapy, 8(4), 315–317.

Drela, K., Stanaszek, L., Nowakowski, A., Kuczynska, Z., & Lukomska, B. (2019). Experimental strategies of mesenchymal stem cell propagation: Adverse events and potential risk of functional changes. Stem Cells International, 2019, 7012692.

Ebihara, L., Acharya, P., & Tong, J. J. (2022). Mechanical stress modulates calcium-activated-chloride currents in differentiating lens cells. Frontiers in Physiology, 31(13), 814651.

Foroozandeh, P., & Aziz, A. A. (2018). Insight into cellular uptake and intracellular trafficking of nanoparticles. Nanoscale Research Letters, 13, 339.

Fraile, M., Eiro, N., Costa, L. A., Martín, A., & Vizoso, F. J. (2022). Aging and mesenchymal stem cells: Basic concepts, challenges and strategies. Biology, 11, 1678.

Garber, J. C., Barbee, R. W., Bielitzki, J. T., Clayton, L. A., Donovan J. C. et al. (2011). Guide for the care and use of laboratory animals. 8th edition. National Research Council (US) Committee for the Update of the Guide for the Care and Use of Laboratory Animals. National Academies Press (US), Washington.

Gimble, J. M., Guilak, F., Nuttall, M. E., Sathishkumar, S., Vidal, M., & Bunnellf, B. A. (2008). *In vitro* differentiation potential of mesenchymal stem cells. Transfusion Medicine and Hemotherapy Journal, 35(3), 228–238.

Guannan Zhu, G., Chen, L., Zeng, F., Gu, L., Yu, X., Li, X., Jiang, J., Guo, G., Cao, J., Tang, K., Zhu, H., Daldrup-Link, H. E., & Wu, M. (2019). $GdVO_4:Eu^{3+}Bi^{3+}$ nanoparticles as a contrast agent for MRI and luminescence bioimaging. ACS Omega, 4(14), 15806–15814.

Han, Y., Dong, Z., Wang, C., Li, Q., Hao, Y., Yang, Z., Zhu, W., Zhang, Y., Liu, Z., & Feng, L. (2022). Ferrous ions doped calcium carbonate nanoparticles potentiate chemotherapy by inducing ferroptosis. Journal of Controlled Release, 348, 346–356.

Iwahashi, N., Ikezaki, M., Nishitsuji, K., Yamamoto, M., Matsuzaki, I., Kato, N., Takaoka, N., Taniguchi, M., Murata, S.-I., Ino, K., & Ihara, Y. (2021). Extracellularly released calreticulin induced by endoplasmic reticulum stress impairs syncytialization of cytotrophoblast model BeWo cells. Cells, 10, 1305.

Jha, A. K., Xu, X., Duncan, R. L., & Jia, X. (2011). Controlling the adhesion and differentiation of mesenchymal stem cells using hyaluronic acid-based, doubly crosslinked networks. Biomaterials, 32(10), 2466–2478.

Jiang, Y., Dey, S., & Matsunami, H. (2014). Calreticulin: Roles in cell-surface protein expression. Membranes, 4, 630–641.

Jiménez-Jiménez, C., Manzano, M., & Vallet-Regí, M. (2020). Nanoparticles coated with cell membranes for biomedical applications. Biology, 9(11), 406.

Jin, Y., Ding, Y., Richards, M., Kaakinen, M., Giese, W., Baumann, E., Szymborska, A., André, R., Nordling, S., Schimmel, L., Akmeriç, E. B., Pena, A., Nwadozi, E., Jamalpour, M., Holstein, K., Sáinz-Jaspeado, M., Bernabeu, M. O., Welsh, M., Gordon, E., Franco, C. A., Vestweber, D., Eklund, L., Gerhardt, H., & Claesson-Welsh, L. (2022). Tyrosine-protein kinase Yes controls endothelial junctional plasticity and barrier integrity by regulating VE-cadherin phosphorylation and endocytosis. Nature Cardiovascular Research, 1, 1156–1173.

Jody, G., Wang, W.-A., Robinson, A., & Michalak, M. (2022). Calreticulin and the heart. Cells, 11(11), 1722.

Kapate, N., Clegg, J. R., & Mitragotri, S. (2021). Non-spherical micro- and nanoparticles for drug delivery: Progress over 15 years. Advanced Drug Delivery Reviews, 177, 113807.

Klochkov, V. K., Malyshenko, A. I., Sedyh, O. O., & Malyukin, Y. V. (2011). Wet-chemical synthesis and characterization of luminescent colloidal nanoparticles: $ReVO_4:Eu^{3+}$ (Re=La, Gd, Y) with rod-like and spindle-like shape. Functional Materials, 18(1), 111–115.

Leroueil, P. R., Hong, S., Mecke, A., Baker Jr., J. R., Orr, B. G., & Banaszak, H. M.-M. (2007). Nanoparticle interaction with biological membranes: Does nanotechnology present a Janus face? Accounts of Chemical Research, 40(5), 335–342.

Li, K., Shen, Q., Xie, Y., You, M., Huang, L., & Zheng, X. (2018). Incorporation of cerium oxide into hydroxyapatite coating protects bone marrow stromal cells against H_2O_2-induced inhibition of osteogenic differentiation. Biological Trace Element Research, 182(1), 91–104.

Liang, Y., Liang, N., Yin, L., & Xiao, F. (2020). Cellular and molecular mechanisms of xenobiotics-induced premature senescence. Toxicology Research, 9(5), 669–675.

Linxia Zhang, L., & Chan, C. (2010). Isolation and enrichment of rat mesenchymal stem cells (MSCs) and separation of single-colony derived MSCs. The Journal of Visualized Experiments, 37, 852.

Lu, H., Guo, L., Kawazoe, N., Tateishi, T., & Chen, G. (2009). Effects of poly(L-lysine), poly(acrylic acid) and poly(ethylene glycol) on the adhesion, prolifera-

tion and chondrogenic differentiation of human mesenchymal stem cells. Journal of Biomaterials Science (Polymer Edition), 20(5–6), 577589,
Lu, Y., Yang, Y., Liu, S., & Ge, S. (2022). Biomaterials constructed for MSC-derived extracellular vesicle loading and delivery – a promising method for tissue regeneration. Frontiers in Cell and Developmental Biology, 10, 898394.
Maker, A., Bolejack, M., Schecterson, L., Hammerson, B., Abendroth, J., Edwards, T. E., Staker, B., Myler, P. J., & Gumbiner, B. M. (2022). Regulation of multiple dimeric states of E-cadherin by adhesion activating antibodies revealed through Cryo-EM and X-ray crystallography. PNAS Nexus, 1(4), 163.
Manzanares, D., & Ceña, V. (2020). Endocytosis: The nanoparticle and submicron nanocompounds gateway into the cell. Pharmaceutics, 12(4), 371.
Mao, A. S., Shin, J.-W., & Mooney, D. J. (2016). Effects of substrate stiffness and cell-cell contact on mesenchymal stem cell differentiation. Biomaterials, 98, 181–191.
Mareschi, K., Rustichelli, D., Calabrese, D., Gunetti, M., Sanavio, F., Castiglia, S., Risso, A., Ferrero, I., Tarella, C., & Fagioli, F. (2012). Multipotent mesenchymal stromal stem cell expansion by plating whole bone marrow at a low cellular density: A more advantageous method for clinical use. Stem Cells International, 2012, 920581.
Mathieu, M., Vigier, S., Labour, M. N., Jorgensen, C., Belamie, E., & Noel, D. (2014). Induction of mesenchymal stem cell differentiation and cartilage formation by cross-linker-free collagen microspheres. European Cells and Materials, 28, 82–96.
Matuła, K., Richter, Ł., Adamkiewicz, W., & Holyst, R. (2016). Influence of nanomechanical stress induced by ZnO nanoparticles of different shape on viability of cells. Soft Matter, 12(18), 4162–4169.
Miyoshi, H., & Adachi, T. (2014). Topography design concept of a tissue engineering scaffold for controlling cell function and fate through actin cytoskeletal modulation. Tissue Engineering Reviews (Part B), 20(6), 609–627.
Montel, L., Guigue, Q., & Pontani, L.-L. (2022). Adhesion regulation and the control of cellular rearrangements: From emulsions to developing tissues. Frontiers in Physics, 10, 1014428.
Muraya, K., Kawasaki, T., Yamamoto, T., & Akutsu, H. (2019). Enhancement of cellular adhesion and proliferation in human mesenchymal stromal cells by the direct addition of recombinant collagen i peptide to the culture medium. BioResearch Open Access, 22, 8(1), 210–218.
Natarajan, D., Ye, Z., Wang, L., Ge, L., & Pathak, J. L. (2021). Rare earth smart nanomaterials for bone tissue engineering and implantology: Advances, challenges, and prospects. Bioengineering and Translational Medicine, 7(1), e10262.
Netanya, Y. S., & Engelhardt, J. F. (2014). The basic biology of redoxosomes in cytokine-mediated signal transduction and implications for disease-specific therapies. Biochemistry, 53(10), 1551–1564.
Owusu, B. Y., Zimmerman, K. A., & Murphy-Ullrich, J. E. (2018). The role of the endoplasmic reticulum protein calreticulin in mediating TGF-β-stimulated extracellular matrix production in fibrotic disease. The Journal of Cell Communication and Signaling, 12(1), 289–299.
Pakulova, O. K., Klochkov, V. K., Kavok, N. S., Kostina, I. A., Sopotova, A. S., & Bondarenko, V. A. (2017). Effect of rare-earth-based nanoparticles on the erythrocyte osmotic adaptation. Biophysical Bulletin, 37(1), 42–50.
Palmgren, M., & Morsomme, P. (2019). The plasma membrane H^+-ATPase, a simple polypeptide with a long history. Yeast, 36(4), 201–210.
Pan, Y., Shi, L. Z., Yoon, C. W., Preece, D., Gomez-Godinez, V., Lu, S., Carmona, C., Woo, S. H., Chien, S., Berns, M. W., Liu, L., & Wang, Y. (2022). Mechanosensor Piezo1 mediates bimodal patterns of intracellular calcium and FAK signaling. EMBO Journal, 41(17), e111799.
Pastore, C. (2021). Size-dependent nano–bio interactions. Nature Nanotechnology, 16, 1052.
Prokopiuk, V. Y., Tkachenko, A. S., Onishchenko, A. I., Yefimova, S. L., Maksimchuk, P. O., Lazurenko, V. V., & Klochkov, V. K. (2022). $LaVO_4:Eu^{3+}$ nanoparticles show no genotoxicity on fibroblast cultures. In: Nanotechnology and nanomaterials (NANO-2022). Abstract book of participants of the International research and practice conference, 25–27 August 2022. Lviv, LLC APF polygraph service. P. 238.
Robert, A., W., Marcon, B., H., Dallagiovanna, B., & Shigunov, P. (2020). Adipogenesis, osteogenesis, and chondrogenesis of human mesenchymal stem/stromal cells: A comparative transcriptome approach. Frontiers in Cell and Developmental Biology, 8, 561.
Sabourian, P., Yazdani, G., Ashraf, S. S., Frounchi, M., Mashayekhan, S., Kiani, S., & Kakkar, A. (2020). Effect of physico-chemical properties of nanoparticles on their intracellular uptake. International Journal of Molecular Sciences, 21(21), 8019.
Sau, T. P., & Goia, D. (2012). Biomedical application of gold nanoparticles. In: Matijević, E. (Ed). Fine particles in medicine and pharmacy. Springer, New York. Pp. 101–145.
Shang, L., Nienhaus, K., & Nienhaus, G. U. (2014). Engineered nanoparticles interacting with cells: Size matters. Journal of Nanobiotechnology 12(5), 24491160.
Shariatzadeh, S., Moghimi, N., Khalafi, F., Shafiee, S., Mehrabi, M., Ilkhani, S., Tosan, F., Nakhaei, P., Alizadeh, A., Varma, R. S., & Taheri, M. (2022). Metallic nanoparticles for the modulation of tumor microenvironment: A new horizon. Frontiers in Bioengineering and Biotechnology, 10, 847433.
Shin, T. H., Lee, D. Y., Ketebo, A. A., Lee, S., Manavalan, B., Basith, S., Ahn, C., Kang, S. H., Park, S., & Lee, G. (2019). Silica-coated magnetic nanoparticles decrease human bone marrow-derived mesenchymal stem cell migratory activity by reducing membrane fluidity and impairing focal adhesion. Nanomaterials, 9(10), 1475.
Tang, J., Peng, R., & Ding, J. (2010). The regulation of stem cell differentiation by cell-cell contact on micropatterned material surfaces. Biomaterials, 31(9), 2470–2476.
Tkacheva, T. N., Yefimova, S. L., Klochkov, V. K., Borovoy, I. A., & Malyukin, Y. V. (2014). Spectroscopic study of ordered hybrid complexes formation between dye aggregates and $ReVO_4:Eu^{3+}$ (Re = Y, Gd, La) nanoparticles. Journal of Molecular Liquids, 199, 244–250.
Wang, X.-L., Nakamoto, T., Dulinska-Molak, I., Kawazoe, N., & Chen, G.-P. (2016). Regulating the stemness of mesenchymal stem cells by tuning micropattern features. Journal of Materials Chemistry (B), 4(1), 37–45.
Wang, Z., Ruan, J., & Cui, D. (2009). Advances and prospect of nanotechnology in stem cells. Nanoscale Research Letters, 4(7), 593–605.
Xu, J.-J., Zhang, W.-C., Guo, Y.-W., Chen, X.-Y., & Zhange, Y.-N. (2022). Metal nanoparticles as a promising technology in targeted cancer treatment. Drug Delivery, 29(1), 664–678.
Xue, R., Li, J.-Y., Yeh, Y., & Chien, S. (2013). Effects of matrix elasticity and cell density on human mesenchymal stem cells differentiation. The Journal of Orthopaedic Research, 31(9), 1360–1365.
Yaman, S., Chintapula, U., Rodriguez, E., Ramachandramoorthy, H., & Nguyen, K.-T. (2020). Cell-mediated and cell membrane-coated nanoparticles for drug delivery and cancer therapy. Cancer Drug Resistance, 3(4), 879–911.
Yamazaki, M., Kojima, H., & Miyoshi, H. (2020). Morphology and differentiation of human mesenchymal stem cells cultured on a nanoscale structured substrate. Electronics and Communications in Japan, 103(9), 23–28.
Yang, Y.-H. K., Ogando, C. R., See, C. W., Chang, T.-Y., & Barabino, G. A. (2018). Changes in phenotype and differentiation potential of human mesenchymal stem cells aging in vitro. Stem Cell Research and Therapy, 9, 131.
Ye, P., Ye, Y., Chen, X., Zou, H., Zhou, Y., Zhao, X., Chang, Z., Han, B., & Kong, X. (2020). Ultrasmall Fe_3O_4 nanoparticles induce S-phase arrest and inhibit cancer cells proliferation. Nanotechnology Reviews, 9(1), 61–69.
Yeo, G. C., & Weiss, A. S. (2019). Soluble matrix protein is a potent modulator of mesenchymal stem cell performance. Proceedings of the National Academy of Sciences of the USA, 116(6), 2042–2051.
Yui, A., Caaveiro, J.-M.-M., Kuroda, D., Nakakido, M., Nagatoishi, S., Goda, S., Maruno, T., Uchiyama, S., & Tsumoto, K. (2021). Mechanism of dimerization and structural features of human LI-cadherin. The Journal of Biological Chemistry, 297(3), 101054.
Zhang, Y., Qin, Z., Qu, Z., Ge, M., & Yang, J. (2020). Cadherin-based biomaterials: Inducing stem cell fate towards tissue construction and therapeutics. Progress in Natural Science: Materials International, 30(5), 597–608.
Zhao, A. G., Shah, K., Freitag, J., Cromer, B., & Sumer, H. (2020). Differentiation potential of early- and late-passage adipose-derived mesenchymal stem cells cultured under hypoxia and normoxia. Stem Cells International, 2020, 8898221.
Zhou, M., Li, B., Li, N., Li, M., & Xing, C. (2022). Regulation of Ca^{2+} for cancer cell apoptosis through photothermal conjugated nanoparticles. ACS Applied Bio Materials, 5(6), 2834–2842.